

# A patch that imparts unconditional stability to certain explicit integrators for SDEs

Nawaf Bou-Rabee\*      Eric Vanden-Eijnden†

October 31, 2018

## Abstract

This paper proposes a simple strategy to simulate stochastic differential equations (SDE) arising in constant temperature molecular dynamics. The main idea is to patch an explicit integrator with Metropolis accept or reject steps. The resulting ‘Metropolized integrator’ preserves the SDE’s equilibrium distribution and is pathwise accurate on finite time intervals. As a corollary the integrator can be used to estimate finite-time dynamical properties along an infinitely long solution. The paper explains how to implement the patch (even in the presence of multiple-time-stepsizes and holonomic constraints), how it scales with system size, and how much overhead it requires. We test the integrator on a Lennard-Jones cluster of particles and ‘dumbbells’ at constant temperature.

**Keywords** molecular dynamics, Metropolis-Hastings, Verlet, RATTLE, RESPA

**AMS Subject Classification** 82C80 (65C30, 65C05, 65P10)

---

\*Courant Institute of Mathematical Sciences, New York University, 251 Mercer Street, New York, NY 10012-1185 (nawaf@cims.nyu.edu). N. B-R. was supported by NSF Fellowship # DMS-0803095.

†Courant Institute of Mathematical Sciences, New York University, 251 Mercer Street, New York, NY 10012-1185 (eve2@cims.nyu.edu). The work of E. V.-E. was supported in part by NSF grants DMS-0718172 and DMS-0708140, and ONR grant N00014-04-1-6046.

# 1 Introduction

**Motivation** Since Loup Verlet’s landmark paper in 1967, the classical Verlet algorithm has been the main workhorse for constant energy molecular dynamics [53]. It is an attractive algorithm for the Hamiltonian ODEs that arise in this context because of its explicit, time-reversible, and symplectic nature. In particular, symplecticity implies long time stability of the Verlet algorithm. The usual proof of this statement uses backward error analysis to show that level sets of a nearby Hamiltonian function interpolate Verlet trajectories [4, 36, 37]. This property implies that a Verlet trajectory is confined to these level sets for the duration of the simulation. As a consequence a Verlet integrator nearly preserves the true energy and exhibits linear growth in global error. Versions of Verlet to constrained (RATTLE) and multiscale (RESPA) Hamiltonian systems are also available. For these reasons Verlet integrators are well-suited for long time simulation of constant energy molecular dynamics.

The situation is quite different in the context of constant temperature molecular dynamics. A molecular system at constant temperature visits every energy isosurface with nonzero probability and its evolution is typically modeled using ergodic stochastic differential equations (SDE). In contrast to their deterministic counterpart, explicit integrators for SDEs diverge from the equilibrium behavior of the true solution [9]. This divergence is easy to understand since explicit integrators are only *conditionally* stable. Indeed for any time-stepsize one can find an energy above which an explicit integrator is unstable. As a result stochastic effects necessarily induce instabilities by driving trajectories to these energy values. Since molecular simulations often involve unbounded potential energy (e.g., Lennard-Jones interaction), these energy values are attainable, and this issue calls for new integration strategies for constant temperature molecular dynamics.

**Constant Temperature Molecular Dynamics** We briefly recall what it means for a molecular system to be at constant temperature. Consider  $n$  molecules with masses  $m_i$  for  $i = 1, \dots, n$  evolving in a  $d$ -dimensional periodic box (or torus in  $\nu = dn$  dimensions  $\mathbb{T}^\nu$ ). Let  $M$  represent the diagonal mass matrix of the molecular system. We assume the particle interaction is given by a potential energy function  $U : \mathbb{T}^\nu \rightarrow \mathbb{R}$ . The Hamiltonian  $H : \mathbb{T}^\nu \times \mathbb{R}^\nu \rightarrow \mathbb{R}$  of this system can be written as:

$$H(\mathbf{q}, \mathbf{p}) = \frac{1}{2} \mathbf{p}^T \mathbf{M}^{-1} \mathbf{p} + U(\mathbf{q}), \quad (1)$$

where  $\mathbf{q} \in \mathbb{T}^\nu$  and  $\mathbf{p} \in \mathbb{R}^\nu$  represent respectively the positions and momenta of the molecules. In terms of this Hamiltonian, define the probability distribution  $\mu$ :

$$\mu(d\mathbf{q}, d\mathbf{p}) \stackrel{\text{def}}{=} Z^{-1} e^{-\beta H(\mathbf{q}, \mathbf{p})} d\mathbf{q} d\mathbf{p} \quad Z = \int_{\mathbb{T}^\nu \times \mathbb{R}^\nu} e^{-\beta H(\mathbf{q}, \mathbf{p})} d\mathbf{q} d\mathbf{p} . \quad (2)$$

Here we have introduced the parameter  $\beta$  which is inversely related to the temperature  $\mathcal{T}$  and Boltzmann constant  $k_B$  via  $\beta = 1/(k_B \mathcal{T})$ .

A molecular system with Hamiltonian (1) is at constant temperature  $\mathcal{T}$  if its trajectories sample from the probability distribution (2). The standard way to guarantee that this is indeed the case is to assume that the molecular system follows a continuous, stochastic dynamics of the form:

$$\begin{cases} \frac{d\mathbf{Q}}{dt} &= \mathbf{M}^{-1} \mathbf{P} , \\ d\mathbf{P} &= -\nabla U(\mathbf{Q}) dt + d\boldsymbol{\eta}(\mathbf{Q}, \mathbf{P}) , \end{cases} \quad (3)$$

where  $d\boldsymbol{\eta} : \mathbb{T}^\nu \times \mathbb{R}^\nu \rightarrow \mathbb{R}^\nu$  represents a thermostat force. Physically one can interpret the thermostat force as modeling interaction between the molecular system and a heat bath. Mathematically it is essential that the thermostat force be stochastic to ensure that the dynamics of (3) be ergodic with respect to (2). Several specific forms of the thermostat force have been proposed in the literature [10, 11, 24, 41, 43] and which one is best remains open for debate. This is a modeling question which is beyond the scope of the present paper. Here we assume that the thermostat force is given, and we propose an integration strategy that does not make strong assumptions on its precise form. In the applications and theory sections of this paper we focus on  $d\boldsymbol{\eta}$  given by Langevin dynamics [10, 43] and in a companion paper [8] consider other thermostats including stochastic rescaling dynamics [11, 12] and Nosé-Hoover-Langevin dynamics [24, 41]. The assumption of continuity excludes, e.g., the Andersen thermostat because it involves discrete collisions at random times that in their wake leave the momentum of the molecular system discontinuous [3]. We refer the reader to [15, 29] for recent progress quantifying the mixing properties of the Andersen thermostat for molecular systems.

The SDE (3) is characterized by degenerate noise, irregular drift, high-dimensionality ( $\nu$  is typically very big), and non-well-separated time-scales. In this context the main aim of numerical methods is to estimate long-time dynamical properties. This calculation is typically done by launching a single run of an explicit integrator and collecting statistics. However, without the patch introduced below this approach is prone to failure due to numerical instabilities.

To be concrete consider computing the time-correlation in momentum along an equilibrium path of the SDE. This computation is common in molecular dynamics and the reader is referred to [2, 18] for expository accounts. Define the continuous equilibrium correlation in momentum as:

$$A(\tau) = \langle \mathbf{P}(\tau + t)^T \mathbf{P}(t) \rangle, \quad (t \geq 0), \quad (\tau \geq 0), \quad (4)$$

where the angle brackets denote a double average with respect to realizations of (3) and an initial condition distributed according to (2). The usual way to estimate  $A(\tau)$  over a time interval  $[0, T]$  is by a sample average computed on-the-fly using a single run of an integrator. The numerical equilibrium correlation is defined as the limit as the number of samples tends to  $\infty$ :

$$A^h(\tau) = \lim_{N \rightarrow \infty} \left( \frac{1}{N} \sum_{k=1}^N \mathbf{P}_{[(\tau+t_k)/h]}^T \mathbf{P}_{[t_k/h]} \right). \quad (5)$$

The difficulty is that this limit does not generally exist if the integrator is explicit. This divergence is an established problem with explicit discretizations of SDEs that possess drifts of limited regularity [22, 35, 46].

**Proposed Integration Strategy** This paper proposes a new integration strategy to solve the SDE (3) based on combining an explicit integrator with Monte Carlo methods to sample from the SDE’s equilibrium distribution [19, 30, 34]. The resulting ‘Metropolized integrator’ preserves the equilibrium distribution and is often provably ergodic. This feature motivates their use as sampling methods [1, 13, 39, 42, 44]. In addition, in [9] we showed that a Metropolized integrator also approximates pathwise the SDE’s solution on finite-time intervals.

These properties ensure that a Metropolized integrator can be used to estimate dynamics along an infinitely long solution of (3). Indeed one can generate a long time trajectory of a Metropolized integrator, and along any finite-time interval update sample averages of dynamic quantities. These averages converge as a consequence of ergodicity of a Metropolized integrator. The averages can also be made arbitrarily close to the true solution’s average by selecting the time-stepsize small enough. For example, a Metropolized integrator can be used to approximate to arbitrary precision the equilibrium correlation function  $A(\tau)$ . In fact, we show in this paper for every  $T > 0$ , there exists a  $C(T) > 0$  such that for  $h$  sufficiently small

$$\sup_{\tau \in [0, T]} |A^h(\tau) - A(h \lfloor \tau/h \rfloor)| \leq C(T)h. \quad (6)$$

The constant  $C(T)$  increases monotonically with the length of the time-interval  $T$ . Hence, one cannot use this integrator in situations where  $T$  is very large like rare event simulation. For such problems the reader is referred to methods adapted to molecular systems with rare events such as milestoning [51, 52].

The error estimate (6) provides a theoretical order of accuracy of a Metropolized integrator. However, for the strategy to be practical, several questions remain:

- what does the patch involve?
- is the patch scalable with respect to system size?
- does the patch work with RATTLE (Verlet with constraints) [50] or RESPA (Verlet with multiple time-step-sizes) [28, 48]?

The aim of this paper is to answer these questions. The paper is organized as follows:

- §2 provides step-by-step instructions on how to patch explicit integrators based on Verlet, RATTLE, and RESPA, and some basic theory explaining why the patch works;
- §3 conducts numerical tests on a Lennard-Jones fluid and ‘dumbbell’ systems;
- §4 contains some conclusions and future improvements.

## 2 Patch

The patch involves splicing an explicit integrator with Metropolis steps. We will show that the resulting integrator possesses the following properties:

- (P1) preservation of the SDE’s equilibrium distribution; and,
- (P2) pathwise accuracy on finite time-intervals.

To illustrate how the patch works, we shall implement it on an explicit integrator based on splitting the SDE (3) into Hamilton’s equations:

$$\begin{cases} \frac{d\mathbf{Q}}{dt} = \mathbf{M}^{-1}\mathbf{P} , \\ \frac{d\mathbf{P}}{dt} = -\nabla U(\mathbf{Q}) , \end{cases} \quad (7)$$

and equations describing the effect of the thermostat:

$$\begin{cases} \frac{d\mathbf{Q}}{dt} &= 0, \\ d\mathbf{P} &= d\boldsymbol{\eta}. \end{cases} \quad (8)$$

The explicit integrator considered is defined as a composition of a step of Verlet for (7) and a step of an approximation to (8) (or vice versa). If Verlet is replaced by an implicit method (e.g., implicit Euler), then the splitting will satisfy property (P2). However, due to discretization error, even an implicit integrator will generally fail to satisfy property (P1) [45–47].

Before we continue let us introduce some notation. Let  $\Omega = \mathbb{T}^\nu \times \mathbb{R}^\nu$  denote the  $2\nu$ -dimensional phase space of the molecular system and  $\mathbf{Y}(t) = (\mathbf{Q}(t), \mathbf{P}(t)) \in \Omega$  denote the true solution of (3) at time  $t \geq 0$  with initial condition  $\mathbf{Y}(0) = \mathbf{x} \in \Omega$ . In what follows we take for granted that this solution exists for all time.

## 2.1 Explicit Integrator

Given a time-stepsize  $h$  and time interval  $T$ , set the number of steps to be  $N = \lfloor T/h \rfloor$  and introduce an evenly-spaced mesh in time  $t_k = hk$  for all  $0 \leq k \leq N$ . Let  $\psi_{t_{k+1}, t_k} : \Omega \rightarrow \Omega$  denote an approximation to the thermostat dynamics (8). This map depends on time because of the stochastic effects in the thermostat. For example, for the Langevin dynamics the thermostat force is given by,

$$d\boldsymbol{\eta} = -\gamma \mathbf{M}^{-1} \mathbf{P} dt + \sqrt{2\gamma\beta^{-1}} d\mathbf{W},$$

where  $\mathbf{W}$  is a  $\nu$ -dimensional Wiener process and  $\gamma$  is a thermostat parameter [10, 43]. In this case (8) are Ornstein-Uhlenbeck equations in momentum whose pathwise unique flow is almost surely:

$$\psi_{t_{k+1}, t_k} : (\mathbf{q}, \mathbf{p}) \mapsto (\mathbf{q}, e^{-\gamma \mathbf{M}^{-1} h} \mathbf{p} + \boldsymbol{\eta}_{t_{k+1}, t_k}), \quad (9)$$

where we have introduced the random vector:

$$\boldsymbol{\eta}_{t_{k+1}, t_k} = \sqrt{2\gamma\beta^{-1}} \int_{t_k}^{t_{k+1}} e^{-\gamma \mathbf{M}^{-1} (t_{k+1} - s)} d\mathbf{W}(s).$$

The map  $\psi_{t_{k+1}, t_k}$  satisfies property (P1). For other SDE-based thermostats an approximate map that satisfies (P1) can be similarly constructed. Notice that this map does not alter the positions of the molecular system.

We introduce a second map  $\hat{\theta}_h : \Omega \rightarrow \Omega$  which approximates (7). Since the Hamiltonian is time-independent, this map depends only on the time-stepsize  $h = t_{k+1} - t_k$ . The patch we introduce below will require that this map is symmetric and volume-preserving [20, 25]. An explicit integrator for (3) is then given by:

$$\hat{\varphi}_{t_{k+1}, t_k} = \psi_{t_{k+1}, t_k} \circ \hat{\theta}_h . \quad (10)$$

The order in (10) does not matter since the integrator's single step accuracy is  $\mathcal{O}(h^2)$  either way. Higher-order accurate or implicit schemes can also be patched, but such integrators may require more computational effort per step. To ensure scalability the map  $\hat{\theta}_h$  in (10) will use Verlet to separately update sets of particles of the molecular system.

To this end we partition the molecular system into  $m$  sets of particles so that each set has  $\nu_j$  degrees of freedom and  $\sum_{j=1}^m \nu_j = \nu$ . Given a time stepsize  $h$  and initial condition  $\mathbf{x} \in \Omega$ , a single step of (10) is defined as:

$$\hat{\mathbf{X}}_1 = \psi_{t_1, t_0} \circ \underbrace{\hat{\theta}_{h, m} \circ \cdots \circ \hat{\theta}_{h, 1}}_{\hat{\theta}_h}(\mathbf{x}) \quad (11)$$

This update gives a numerical approximation to  $\mathbf{Y}(h)$ ,  $\hat{\mathbf{X}}_1 \approx \mathbf{Y}(h)$ . The map  $\hat{\theta}_{h, j}$  is defined as a Verlet update of the position and momentum of the  $j$ th set of molecules fixing the other sets. More precisely given an input

$$\mathbf{x}_0 = ((\mathbf{q}_1, \cdots, \mathbf{q}_m), (\mathbf{p}_1, \cdots, \mathbf{p}_m)) ,$$

where  $(\mathbf{q}_j, \mathbf{p}_j) \in \mathbb{T}^{\nu_j} \times \mathbb{R}^{\nu_j}$ , the map  $\hat{\theta}_{h, j}$  outputs

$$\hat{\theta}_{h, j}(\mathbf{x}_0) = ((\mathbf{q}_1, \cdots, \mathbf{q}_{j-1}, \hat{\mathbf{q}}_j, \mathbf{q}_{j+1}, \cdots, \mathbf{q}_m), (\mathbf{p}_1, \cdots, \mathbf{p}_{j-1}, \hat{\mathbf{p}}_j, \mathbf{p}_{j+1}, \cdots, \mathbf{p}_m)) .$$

Here:

$$\begin{cases} \hat{\mathbf{p}}_{j, \frac{1}{2}} &= \mathbf{p}_j - \frac{h}{2} \nabla_{Q_j} U(\mathbf{q}_1, \cdots, \mathbf{q}_m) , \\ \hat{\mathbf{q}}_j &= \mathbf{q}_j + h \mathbf{M}_j^{-1} \hat{\mathbf{p}}_{j, \frac{1}{2}} , \\ \hat{\mathbf{p}}_j &= \hat{\mathbf{p}}_{j, \frac{1}{2}} - \frac{h}{2} \nabla_{Q_j} U(\mathbf{q}_1, \cdots, \mathbf{q}_{j-1}, \hat{\mathbf{q}}_j, \mathbf{q}_{j+1}, \cdots, \mathbf{q}_m) , \end{cases} \quad (12)$$

where  $\mathbf{M}_j$  is the subset of the global mass matrix  $\mathbf{M}$  associated to the  $j$ th set of particles.

The map  $\hat{\theta}_{h, j}$  is symmetric and volume-preserving on  $\Omega$  since it is a Verlet update with respect to the Hamiltonian (1) restricted to:

$$\begin{aligned} &\{\mathbf{q}_1\} \times \cdots \times \{\mathbf{q}_{j-1}\} \times (\mathbb{T}^{\nu_j}) \times \{\mathbf{q}_{j+1}\} \times \cdots \times \{\mathbf{q}_m\} \times \\ &\{\mathbf{p}_1\} \times \cdots \times \{\mathbf{p}_{j-1}\} \times (\mathbb{R}^{\nu_j}) \times \{\mathbf{p}_{j+1}\} \times \cdots \times \{\mathbf{p}_m\} \subset \Omega . \end{aligned}$$

Even though the composite map  $\hat{\theta}_h$  is a first-order splitting of (7), the one-step error of  $\hat{\theta}_{h,j}$  in preserving energy is  $O(h^3)$  because each of the separate Verlet updates is second-order accurate.

## 2.2 Metropolized Integrator

To derive an integrator that satisfies property (P1), we patch the explicit integrator (11) with Metropolis accept or reject steps as follows. Given the time-stepsize  $h$ , the initial condition  $\mathbf{x} \in \Omega$ , and the uniform random numbers  $\zeta_j \sim U(0, 1)$  for  $1 \leq j \leq m$ , one step of a Metropolized Verlet integrator determines  $\mathbf{X}_1 \approx \mathbf{Y}(h)$  using:

$$\mathbf{X}_1 = \psi_{t_1, t_0} \circ \underbrace{\theta_{h,m} \circ \cdots \circ \theta_{h,1}}_{\theta_h}(\mathbf{x}). \quad (13)$$

Here we have introduced the stochastic maps  $\theta_{h,j} : \Omega \rightarrow \Omega$  which are Metropolized versions of the deterministic updates  $\hat{\theta}_{h,j}$ . Given input

$$\mathbf{x}_0 = ((\mathbf{q}_1, \cdots, \mathbf{q}_m), (\mathbf{p}_1, \cdots, \mathbf{p}_m)),$$

the map  $\theta_{h,j}$  computes a proposed move

$$\mathbf{x}_1^* = ((\mathbf{q}_1, \cdots, \mathbf{q}_{j-1}, \mathbf{q}_j^*, \mathbf{q}_{j+1}, \cdots, \mathbf{q}_m), (\mathbf{p}_1, \cdots, \mathbf{p}_{j-1}, \mathbf{p}_j^*, \mathbf{p}_{j+1}, \cdots, \mathbf{p}_m)).$$

using a Verlet update

$$\begin{cases} \mathbf{p}_{j, \frac{1}{2}}^* &= \mathbf{p}_j - \frac{h}{2} \nabla_{Q_j} U(\mathbf{q}_1, \cdots, \mathbf{q}_m), \\ \mathbf{q}_j^* &= \mathbf{q}_j + h \mathbf{M}_j^{-1} \mathbf{p}_{j, \frac{1}{2}}^*, \\ \mathbf{p}_j^* &= \mathbf{p}_{j, \frac{1}{2}}^* - \frac{h}{2} \nabla_{Q_j} U(\mathbf{q}_1, \cdots, \mathbf{q}_{j-1}, \mathbf{q}_j^*, \mathbf{q}_{j+1}, \cdots, \mathbf{q}_m), \end{cases} \quad (14)$$

and accepts this proposed move with probability

$$1 \wedge \exp(-\beta[H(\mathbf{x}_1^*) - H(\mathbf{x}_0)]). \quad (15)$$

If this proposal is rejected the momentum is reversed. To summarize

$$\theta_{h,j} : \mathbf{x}_0 \mapsto \mathbf{x}_1,$$

with output  $\mathbf{x}_1$  defined as

$$\mathbf{x}_1 = ((\mathbf{q}_1, \cdots, \mathbf{q}_{j-1}, \bar{\mathbf{q}}_j, \mathbf{q}_{j+1}, \cdots, \mathbf{q}_m), (\mathbf{p}_1, \cdots, \mathbf{p}_{j-1}, \bar{\mathbf{p}}_j, \mathbf{p}_{j+1}, \cdots, \mathbf{p}_m)).$$

where

$$(\bar{\mathbf{q}}_j, \bar{\mathbf{p}}_j) = \begin{cases} (\mathbf{q}_j^*, \mathbf{p}_j^*) & \text{if } \zeta_j < 1 \wedge \exp(-\beta[H(\mathbf{x}^*) - H(\mathbf{x})]) , \\ (\mathbf{q}_j, -\mathbf{p}_j) & \text{otherwise .} \end{cases} \quad (16)$$

The patch we propose consists of an accept or reject step like (16). It requires evaluating the total energy at the current step and at the proposed moves. These statistics are usually computed alongside evaluations of the force field. When a proposed move is rejected, the momentum of the  $j$ th set of particles is reversed. While these rejections ensure the integrator is unconditionally stable and preserves the SDE's equilibrium distribution, they cause an  $O(1)$  error in accuracy due to momentum reversals. Next we consider the effect of these rejections and momentum reversals on the approximation to the dynamics of the SDE.

### 2.3 Quantitative Error Estimates

Consider once more the Hamiltonian of the molecular system:

$$H(\mathbf{q}, \mathbf{p}) = \frac{1}{2} \mathbf{p}^T \mathbf{M}^{-1} \mathbf{p} + U(\mathbf{q}) \quad (17)$$

where  $\mathbf{q} \in \mathbb{T}^\nu$  and  $\mathbf{p} \in \mathbb{R}^\nu$  represent a configuration and momentum of the molecular system, respectively. For simplicity, we will assume the thermostat dynamics is given by Langevin [10, 43]:

$$\begin{cases} \frac{d\mathbf{Q}}{dt} &= \mathbf{M}^{-1} \mathbf{P} , \\ d\mathbf{P} &= -\nabla U(\mathbf{Q}) dt - \gamma \mathbf{M}^{-1} \mathbf{P} dt + \sqrt{2\gamma\beta^{-1}} d\mathbf{W} , \end{cases} \quad (18)$$

where  $\gamma$  is a thermostat parameter,  $\beta$  is the ‘inverse temperature’ entering the distribution (2), and  $\mathbf{W}$  is a  $\nu$ -dimensional Wiener process. The theory below will rely on the following regularity of the potential energy.

**Assumption 2.1.** *The potential energy  $U : \mathbb{T}^\nu \rightarrow \mathbb{R}$  is smooth.*

*Remark 2.2.* This assumption does not permit the potential force to have singularities. For example, it holds for Morse potential interactions, but not Lennard-Jones interactions. One can relax this requirement by replacing smoothness of  $U$  by some coercivity.

Let  $\mathbb{E}^\mu$  denote expectation conditioned on the initial distribution being the equilibrium distribution of the SDE (18):

$$\mathbb{E}^\mu(g(\mathbf{X}_k)) = \int_{\Omega} \mathbb{E}^{\mathbf{x}}(g(\mathbf{X}_k)) \mu(d\mathbf{x}), \quad \mathbf{X}_0 = \mathbf{x} \in \Omega .$$

The following theorem states that the Metropolized integrator satisfies property (P2).

**Theorem 2.3.** *Assume 2.1. For every  $T > 0$ , there exist positive constants  $h_c$  and  $C(T)$  such that,*

$$\left( \mathbb{E}^\mu \left\{ \left| \mathbf{X}_{\lfloor t/h \rfloor} - \mathbf{Y}(h \lfloor t/h \rfloor) \right|^2 \right\} \right)^{1/2} \leq C(T)h ,$$

for all  $h < h_c$  and  $t \in [0, T]$ .

A proof of this result relies on single-step accuracy and bounds on moments of the Metropolized integrator (see [9]). These bounds help to boost the single-step error estimate to a global error estimate, and hence, pathwise convergence on finite time-intervals. The Metropolized integrator initiated from equilibrium satisfies such bounds as a consequence of property (P1).

Theorem 2.3 does not require that the Metropolized integrator be ergodic, but only that it preserves the equilibrium distribution. For this reason one can extend this result to Metropolis-adjusted discretizations of other SDE-based thermostats. Ergodicity is technically difficult to establish when the thermostat force is a non-linear function of the state or highly degenerate (see, e.g., [24]). However, for Langevin dynamics (18) with linear friction and additive noise on all momenta, ergodicity is straightforward to establish for the Metropolized integrator.

**Theorem 2.4** (Ergodicity). *Assume 2.1. For all  $h > 0$ , observables  $g : \Omega \rightarrow \mathbb{R}$ , and initial conditions  $\mathbf{x} \in \Omega$ ,*

$$\lim_{T \rightarrow \infty} \frac{1}{T} \int_0^T g(\mathbf{X}_{\lfloor t/h \rfloor}) dt = \int_{\Omega} g(\mathbf{x}) \mu(d\mathbf{x}).$$

where  $\mathbf{X}_0 = \mathbf{x}$ .

*Proof.* This proof is terse. We prove this statement for the Metropolized integrator based on a trivial partition of the molecular system. For more details please see [9] and references therein. The Metropolized integrator by construction satisfies property (P1). Moreover, its acceptance probability is strictly less than one

everywhere, and the integrator without accept or reject steps admits a smooth transition density when sampled every other step. These two observations imply that the smooth part of the two-step transition probability of the Metropolized integrator is supported everywhere, and hence, the chain is irreducible. Irreducibility and property (P1) together imply ergodicity [33].  $\square$

Theorems 2.3 and 2.4 are sufficient to establish that the Metropolized integrator can estimate dynamics along equilibrium trajectories of (18). For example, as a corollary to the above theorems one can prove that the Metropolized integrator can be used to compute equilibrium correlation functions.

**Corollary 2.5.** *Assume 2.1. For every  $T > 0$  there exist positive constants  $h_c$  and  $C(T)$  such that*

$$|A^h(\tau) - A(h\lfloor\tau/h\rfloor)| \leq C(T)h,$$

for all  $h < h_c$  and  $\tau \in [0, T]$ .

A proof of this result is provided in the Appendix.

## 2.4 Case of Multiple-Time-Stepsizes

Now we present an implementation of the patch to an explicit integrator for (3) based on a multiple-time-stepsize integrator known as RESPA [28, 48]. RESPA was proposed for molecular systems at constant energy in [49]. This integrator is a version of Verlet adapted to molecular systems with multiple time scales. It is designed to overcome a time-stepsize restriction imposed by rapidly changing short-range interactions. The scheme evaluates short-range forces on a smaller time-stepsize, and hence, more frequently than long-range forces. The overall accuracy of the algorithm is dictated by the largest time-stepsize. For Hamiltonian ODEs RESPA is known to exhibit resonance instabilities as described in [17]. The resonance occurs between forces evaluated at the coarse time-stepsize and the normal modes of the molecular system excluding long-range interactions. These numerical instabilities also appear in generalizations of RESPA to Langevin SDEs [16, 23, 31]. In the following we show how to patch such a generalization to tackle such instabilities.

Again we partition the molecular system into  $m$  sets of particles so that each set has  $\nu_i$  degrees of freedom and  $\sum_{i=1}^m \nu_i = \nu$ . We assume that the potential energy can be decomposed into fast and slow interactions:

$$U(\mathbf{q}) = U_{\text{slow}}(\mathbf{q}) + U_{\text{fast}}(\mathbf{q}).$$

We further assume fast and slow potential forces are respectively evaluated at  $h_f$  and  $h$  time increments. The small time-stepsize is typically a fraction of the large time-stepsize. The integrator (13) will be used, except that  $\theta_{h,j}$  is replaced with a Metropolized version of RESPA that separately updates each element of the partition. Given a small time-stepsize  $h_f$ , large time-stepsize  $h$ , and input

$$\mathbf{x}_0 = ((\mathbf{q}_1, \dots, \mathbf{q}_m), (\mathbf{p}_1, \dots, \mathbf{p}_m)) .$$

Set  $N_f = \lfloor h/h_f \rfloor$ . The map  $\theta_{h,j}$  computes a proposed move

$$\mathbf{x}_1^* = ((\mathbf{q}_1, \dots, \mathbf{q}_{j-1}, \mathbf{q}_j^*, \mathbf{q}_{j+1}, \dots, \mathbf{q}_m), (\mathbf{p}_1, \dots, \mathbf{p}_{j-1}, \mathbf{p}_j^*, \mathbf{p}_{j+1}, \dots, \mathbf{p}_m)) ,$$

using a RESPA update

$$\left\{ \begin{array}{l} \mathbf{p}_{j, \frac{1}{N_f}} = \mathbf{p}_j - \frac{h}{2} \nabla_{Q_j} U_{\text{slow}}(\mathbf{q}_1, \dots, \mathbf{q}_m) , \\ \mathbf{q}_{j, \frac{1}{N_f}} = \mathbf{q}_j \\ \left\{ \begin{array}{l} \mathbf{P}_{j, \frac{k+1}{N_f}} = \mathbf{p}_{j, \frac{k}{N_f}} - \frac{h_f}{2} \nabla_{Q_j} U_{\text{fast}}(\mathbf{q}_1, \dots, \mathbf{q}_{j-1}, \mathbf{q}_{j, \frac{k}{N_f}}, \mathbf{q}_{j+1}, \dots, \mathbf{q}_m) , \\ \mathbf{q}_{j, \frac{k+1}{N_f}} = \mathbf{q}_{j, \frac{k}{N_f}} + h_f \mathbf{M}_j^{-1} \mathbf{P}_{j, \frac{k+1}{N_f}} , \\ \mathbf{p}_{j, \frac{k+1}{N_f}} = \mathbf{P}_{j, \frac{k+1}{N_f}} - \frac{h_f}{2} \nabla_{Q_j} U_{\text{fast}}(\mathbf{q}_1, \dots, \mathbf{q}_{j-1}, \mathbf{q}_{j, \frac{k+1}{N_f}}, \mathbf{q}_{j+1}, \dots, \mathbf{q}_m) , \end{array} \right. \\ \mathbf{q}_j^* = \mathbf{q}_{j,1} \\ \mathbf{p}_j^* = \mathbf{p}_{j,1} - \frac{h}{2} \nabla_{Q_j} U_{\text{slow}}(\mathbf{q}_1, \dots, \mathbf{q}_{j-1}, \mathbf{q}_j^*, \mathbf{q}_{j+1}, \dots, \mathbf{q}_m) , \end{array} \right.$$

where the inner index  $k$  runs from  $1, \dots, N_f - 1$  (where  $N_f$  is the number of steps taken at the small time-stepsize  $h_f$ ) and the outer index  $j$  runs from  $1, \dots, m$  (where  $m$  is the number of elements in the partition). This proposed move is accepted with probability

$$1 \wedge \exp(-\beta[H(\mathbf{x}_1^*) - H(\mathbf{x}_0)]) . \quad (19)$$

If this proposal is rejected the momentum is reversed as before. This generalization of RESPA achieves a speedup when the slow potential force is expensive to evaluate relative to the fast potential force.

## 2.5 Case of Holonomic Constraints

Here we show how to implement the patch to molecular systems with holonomic constraints. Similar issues are treated in [21, 27] from the viewpoint of sampling

in the presence of constraints. Again we partition the molecular system with mass matrix  $M$  into  $m$  sets of particles so that each set has  $\nu_i$  degrees of freedom and  $\sum_{i=1}^m \nu_i = \nu$ . The main difference to the previous cases is the possibility that the dynamics along each element of this partition is not well-defined. For instance, if the constraint couples all atoms in the molecule, then only the trivial partition will lead to well-posed dynamics. Or, if the constraint couples pairs of molecules, then only partitions in terms of these pairs are permissible.

To rule out this possibility, we assume that the  $j$ th set of the partition has an associated scalar constraint function  $g_j : \mathbb{T}^\nu \rightarrow \mathbb{R}$  independent from the positions of the other sets. The case of vectorial constraints can be handled quite similarly, but for clarity we will consider scalar constraints here. The intersection of the zero level sets of these constraint functions defines the constraint manifold  $\Sigma = \cap_{i=1}^m g_i^{-1}(0) \subset \Omega$ . The velocities of the constrained atoms are tangent to this manifold. These observations motivate introducing the set of all constrained positions and momenta denoted by  $T\Sigma$  which is known as the cotangent manifold:

$$T\Sigma = \{(\mathbf{q}, \mathbf{p}) \in \Omega \mid g_i(\mathbf{q}) = 0, \nabla_{\mathbf{Q}_i} g_i(\mathbf{q})^T \mathbf{M}_i^{-1} \mathbf{p}_i = 0, i = 1, \dots, m\},$$

where  $M_i$  is the subset of the global mass matrix  $M$  associated to the  $i$ th set of particles.

For a molecular system with constraints, the probability distribution (2) is replaced by:

$$d\mu_{T\Sigma}(\mathbf{q}, \mathbf{p}) \stackrel{\text{def}}{=} Z^{-1} e^{-\beta H(\mathbf{q}, \mathbf{p})} d\sigma_{T\Sigma}(\mathbf{q}, \mathbf{p}), \quad Z = \int_{T\Sigma} e^{-\beta H(\mathbf{q}, \mathbf{p})} d\sigma_{T\Sigma}(\mathbf{q}, \mathbf{p}). \quad (20)$$

Here the measure  $\sigma_{T\Sigma}$  represents standard volume measure on the manifold  $T\Sigma$ . Introduce the Lagrange multiplier  $\lambda_i(t) \in \mathbb{R}$ . The stochastic dynamics of the constrained molecular system is assumed to be of the form:

$$\begin{cases} \frac{d\mathbf{Q}_i}{dt} &= \mathbf{M}_i^{-1} \mathbf{P}_i, \\ d\mathbf{P}_i &= -\nabla_{\mathbf{Q}_i} U(\mathbf{Q}) dt + \nabla_{\mathbf{Q}_i} g_i(\mathbf{Q}) d\lambda_i + d\boldsymbol{\eta}_i(\mathbf{Q}, \mathbf{P}), \\ g_i(\mathbf{Q}) &= 0, \end{cases} \quad (21)$$

where  $i$  enumerates the elements in the partition. To check that (20) is an invariant measure of (21), it suffices to show its density is a stationary solution of the corresponding Fokker-Planck equation. We will assume the solution to (21) is ergodic with respect to the probability distribution  $\mu_{T\Sigma}$ . To eliminate the Lagrange multiplier appearing in (21), ‘differentiate’ the constraint function twice along a

path of  $(\mathbf{Q}, \mathbf{P})$  following either the heuristic approach in [50] or the rigorous approach described in [7, 14].

We will now introduce a constrained version of (11). It is obtained by splitting (21) into a constrained Hamiltonian system:

$$\begin{cases} \frac{d\mathbf{Q}_i}{dt} &= \mathbf{M}_i^{-1} \mathbf{P}_i, \\ \frac{d\mathbf{P}_i}{dt} &= -\nabla_{\mathbf{Q}_i} U(\mathbf{Q}) + \nabla_{\mathbf{Q}_i} g_i(\mathbf{Q}) \lambda_{i,1}, \\ g_i(\mathbf{Q}) &= 0, \end{cases} \quad (22)$$

and constrained thermostat dynamics:

$$\begin{cases} \frac{d\mathbf{Q}_i}{dt} &= 0, \\ d\mathbf{P}_i &= d\boldsymbol{\eta}_i + \nabla_{\mathbf{Q}_i} g_i(\mathbf{Q}) d\lambda_{i,2}, \\ 0 &= \nabla_{\mathbf{Q}_i} g_i(\mathbf{Q})^T \mathbf{M}_i^{-1} \mathbf{P}_i. \end{cases} \quad (23)$$

We approximate the solution to (22) by using a constrained version of Verlet known as RATTLE [40]. As before to maintain scalability we will separately propagate each set of the partition using RATTLE. Since RATTLE moves are time-reversible and volume-preserving [26], a Metropolis method based on a RATTLE proposed move and the probability distribution (20) yields an acceptance probability that is a function of the change in energy induced by the separate RATTLE moves. As before we compose this map with an approximation to (23) which we denote by  $\psi_{t_{k+1}, t_k} : T\Sigma \rightarrow T\Sigma$ . The step-by-step procedure to implement this algorithm is given below.

If we assume that the thermostat in (23) is given by Langevin dynamics, then its pathwise unique flow is given by:

$$\psi_{t_{k+1}, t_k} : \{(\mathbf{q}_i, \mathbf{p}_i)\}_{i=1}^m \mapsto \{(\mathbf{q}_i, e^{-\gamma \mathbb{P}_i(\mathbf{q}) \mathbf{M}_i^{-1} h} \mathbf{p}_i + \boldsymbol{\eta}_{t_{k+1}, t_k}^i)\}_{i=1}^m, \quad (24)$$

where we have introduced the random vector:

$$\boldsymbol{\eta}_{t_{k+1}, t_k}^i = \sqrt{2\gamma\beta^{-1}} \int_{t_k}^{t_{k+1}} e^{-\gamma \mathbb{P}_i(\mathbf{q}) \mathbf{M}_i^{-1} (t_{k+1}-s)} \mathbb{P}_i(\mathbf{q}) d\mathbf{W}_i(s),$$

and the projection matrix:

$$\mathbb{P}_i(\mathbf{q}) = \mathbf{I} - (\nabla_{\mathbf{Q}_i} g_i) [(\nabla_{\mathbf{Q}_i} g_i)^T \mathbf{M}_i^{-1} (\nabla_{\mathbf{Q}_i} g_i)]^{-1} (\nabla_{\mathbf{Q}_i} g_i)^T \mathbf{M}_i^{-1}.$$

Here  $\mathbf{I}$  is the  $\nu_i \times \nu_i$  identity matrix. To derive (24) eliminate the Lagrange multiplier in (23) by differentiating the momentum constraint and using as an integrating factor the matrix  $\exp(\gamma \mathbb{P}_i(\mathbf{q}) \mathbf{M}_i^{-1} t)$ .

*Remark 2.6.* When the mass matrix is not the identity, (24) requires computing the exponential of a position dependent matrix. This calculation is non-trivial, and can be avoided by using SHAKE in place of RATTLE and an unconstrained Ornstein-Uhlenbeck update in place of (24). The resulting Metropolized integrator will satisfy property (P1) with respect to a constrained equilibrium distribution, but with unconstrained velocities. It will also satisfy property (P2).

Given a time-stepsize  $h$ , initial condition  $\mathbf{x} \in \Omega$ , and uniform random numbers  $\zeta_j \sim U(0, 1)$  for  $j = 1, \dots, m$ , one step of the Metropolized integrator determines  $\mathbf{X}_1$  using (13), but with the proposed moves in  $\theta_{h,j}$  obtained by RATTLE as follows. Introduce the discrete Lagrange multipliers  $\lambda_{j,1}, \lambda_{j,2} \in \mathbb{R}$ . The integrator inputs a point in phase space on the constraint manifold

$$\mathbf{x}_0 = ((\mathbf{q}_1, \dots, \mathbf{q}_m), (\mathbf{p}_1, \dots, \mathbf{p}_m)),$$

and outputs a proposed move on the constraint manifold

$$\mathbf{x}_1^* = ((\mathbf{q}_1, \dots, \mathbf{q}_{j-1}, \mathbf{q}_j^*, \mathbf{q}_{j+1}, \dots, \mathbf{q}_m), (\mathbf{p}_1, \dots, \mathbf{p}_{j-1}, \mathbf{p}_j^*, \mathbf{p}_{j+1}, \dots, \mathbf{p}_m)),$$

where  $(\mathbf{q}_j^*, \mathbf{p}_j^*)$  are determined by

$$\begin{cases} \mathbf{p}_{j,\frac{1}{2}}^* &= \mathbf{p}_j - \frac{h}{2} \nabla_{Q_j} U(\mathbf{q}_1, \dots, \mathbf{q}_m) - \frac{h}{2} \lambda_{j,1} \nabla_{Q_j} g_j(\mathbf{q}_1, \dots, \mathbf{q}_m), \\ \mathbf{q}_j^* &= \mathbf{q}_j + h \mathbf{M}_j^{-1} \mathbf{p}_{j,\frac{1}{2}}^*, \\ \mathbf{p}_j^* &= \mathbf{p}_{j,\frac{1}{2}}^* - \frac{h}{2} \nabla_{Q_j} U(\mathbf{q}_1, \dots, \mathbf{q}_{j-1}, \mathbf{q}_j^*, \mathbf{q}_{j+1}, \dots, \mathbf{q}_m) \\ &\quad - \frac{h}{2} \lambda_{j,2} \nabla_{Q_j} g_j(\mathbf{q}_1, \dots, \mathbf{q}_{j-1}, \mathbf{q}_j^*, \mathbf{q}_{j+1}, \dots, \mathbf{q}_m), \\ 0 &= g_j(\mathbf{q}_1, \dots, \mathbf{q}_{j-1}, \mathbf{q}_j^*, \mathbf{q}_{j+1}, \dots, \mathbf{q}_m), \\ 0 &= \nabla_{Q_j} g_j(\mathbf{q}_1, \dots, \mathbf{q}_{j-1}, \mathbf{q}_j^*, \mathbf{q}_{j+1}, \dots, \mathbf{q}_m)^T \mathbf{M}_j^{-1} \mathbf{p}_j^*. \end{cases} \quad (25)$$

The Lagrange multiplier  $\lambda_{j,1}$  enforces that the  $j$ th proposed positions satisfy the position constraint, and  $\lambda_{j,2}$  enforces that the  $j$ th proposed velocities are tangent to the constraint manifold. This proposed move is accepted with probability

$$1 \wedge \exp(-\beta[H(\mathbf{x}_1^*) - H(\mathbf{x}_0)]). \quad (26)$$

This acceptance probability is a function of the change in energy induced by the RATTLE proposed move. If this proposal is rejected the velocity is reversed, but remains tangent to the constraint manifold.

### 3 Applications

This section tests the Metropolized integrators introduced in §2.

#### 3.1 Lennard-Jones Fluid

A Lennard-Jones fluid consists of  $n$  identical particles with pairwise interactions given by a Lennard-Jones potential energy. In what follows we use dimensionless units to describe this system. In these units mass is rescaled by the mass of an individual particle (so that the particles have unit mass), energy by the depth of the Lennard-Jones potential energy, and length by the point where the potential energy is zero. We follow the notation and setup provided in Part I of [18].

We simulate the Lennard-Jones fluid in a fixed periodic box which we call the simulation box. We used a truncated version of the Lennard-Jones potential in which the energy between two particles a distance  $r$  apart is kept constant after a certain cutoff distance and is given by:

$$U_{LJ}(r) = \begin{cases} f(r) - f(r_c) & r < r_c, \\ 0 & \text{otherwise,} \end{cases} \quad (27)$$

where we have introduced  $f(r) = 4(1/r^{12} - 1/r^6)$  and  $r_c$  is bounded above by the size of the simulation box. Other shifts can be used to make the higher derivatives of  $U_{LJ}$  continuous. The error introduced by the truncation in (27) is proportional to the density of the molecular system and can be made arbitrarily small by selecting the cutoff distance sufficiently large.

The pair potentials are a function of the distance between the  $i$ th and  $j$ th particle. If the position of the  $i$ th and  $j$ th particles are  $\mathbf{q}_i$  and  $\mathbf{q}_j$ , and the length of the simulation box  $\ell$ , then this distance is given by:

$$r_{i,j}(\mathbf{q}) = |(\mathbf{q}_i - \mathbf{q}_j) \bmod \ell|.$$

In terms of this pairwise distance, the potential energy of a Lennard-Jones fluid is a sum of interactions between all pairs of particles:

$$U(\mathbf{q}) = \sum_{i=1}^{n-1} \sum_{j=i+1}^n U_{LJ}(r_{i,j}(\mathbf{q})). \quad (28)$$

Evaluating the potential force requires  $O(n^2)$  operations (where  $\nu$  is the dimension of configuration space), and typically dominates total computation cost.

### 3.2 Autocorrelation of Lennard-Jones Fluid

Here we test the accuracy of the Metropolized integrator (13) based on trivial and per particle partitions of the molecular system. In the former proposed moves in the Metropolis steps are obtained by per particle Verlet updates, and in the latter by global Verlet updates. The numerics indicate that the order of accuracy of both methods is roughly  $O(h^2)$  and that the error constant of the per particle partition is approximately an order of magnitude smaller.

To test accuracy we use the Metropolized integrator to estimate the equilibrium momentum autocorrelation of the Lennard-Jones fluid. For the numerical experiment, we set the fluid's density  $\rho = 0.8442$  and temperature  $\mathcal{T} = 0.728$  (units are dimensionless as described earlier). For these values the phase of the Lennard-Jones fluid is liquid, and close to the triple (gas-liquid-solid) point. We also fix the number of particles to be  $n = 25$  and the degrees of freedom to be  $d = 2$ . The size of the simulation box is  $\ell = (n/\rho)^{1/2} \approx 5.04$ . A reasonable cutoff distance in (27) at the selected density is  $r_c = 2.5$ . The initial positions of the particles are chosen to be the vertices of a square lattice that fills the simulation box. For instance, the length of each square in the lattice can be chosen to be  $\ell/\lceil n^{1/2} \rceil$ . The initial velocities are sampled from the Maxwell distribution. The thermostat parameter is set equal to  $\gamma = 1.0$ .

In the simulations we estimate the true velocity autocorrelation over a time-interval  $[0, 1]$ . Set  $N = \lfloor T/h \rfloor$  and introduce an evenly-spaced mesh in computational time  $t_k = hk$  for all  $0 \leq k \leq N$ . Let  $A^h : [0, 1] \rightarrow \mathbb{R}$  denote the velocity correlation function obtained by the Metropolized integrator (13):

$$A^h(\tau) = \lim_{N \rightarrow \infty} \frac{1}{N} \sum_{k=1}^N \mathbf{P}_{\lfloor (\tau+t_k)/h \rfloor}^T \mathbf{P}_{\lfloor t_k/h \rfloor}, \quad (\tau \geq 0).$$

Define the relative Richardson error as

$$\epsilon_h \stackrel{\text{def}}{=} \frac{\sup_{\tau \in [0,1]} |A^h(\tau) - A^{2h}(\tau)|}{\sup_{\tau \in [0,1]} |A(\tau)|}. \quad (29)$$

An empirical estimate of  $\epsilon_h$  is plotted for time-stepsizes

$$h = \{0.005, 0.0025, 0.00125, 0.000625\}$$

in Fig. 1 with  $N = 10^8$ . The denominator in  $\epsilon_h$  is calculated by using the approximation of  $A$  at  $h = 0.000625$ . The figure shows that the error of the Metropolized

integrator is approximately  $O(h^2)$ . Moreover it shows that the Metropolized integrator based on a per particle partition is nearly an order of magnitude more accurate than the algorithm based on a trivial partition.

### 3.3 Scaling of Metropolized Integrator

Until now the numerics dealt with a fixed number of particles in  $d = 2$  dimensions. Next we address how the integrator (13) scales with the number of particles keeping the density and temperature fixed. As before we consider two types of partitions: per particle and trivial. This time we will assume the particles are in three-dimensional space. Recall that in the former proposed moves in the Metropolis steps are obtained by per particle Verlet updates, and in the latter by global Verlet updates. We will show that the type of proposed move affects the scalability of the Metropolized integrator. In particular, the per particle partition will lead to a scalable algorithm.

By fixing the density and temperature, the stiffness of the molecular system is fixed. Thus, from the viewpoint of numerical analysis, the time-stepsize ought to be independent of system size. However, the acceptance probability in the Metropolized integrator depends on the change in energy induced by the proposal move (see (15)). If this proposal move is global, then the magnitude of this change in energy increases with system size. Hence, the acceptance probability is inversely related to system size, in general. This poor scaling of Metropolis methods based on global moves is well-known in the literature (see, e.g., [5, 32, 38]).

For the numerical experiment, we set the fluid's density  $\varrho = 0.8442$  and temperature  $\mathcal{T} = 0.728$  (as before units are dimensionless). The mean acceptance probability is computed along a long time trajectory of the integrators ( $10^6$  steps) with a fixed time-stepsize of  $h = 0.01$  and a variety of system sizes. The initial positions of the particles are the vertices of a cubic lattice contained in the simulation box. The length of each cube is given by  $\lceil (1/\varrho)^{1/3} \rceil$  ( $\varrho = 0.8442$  is the density of the fluid). The initial velocities are sampled from the Maxwell distribution. The thermostat parameter and Lennard-Jones cutoff distances are set equal to  $\gamma = 1.0$  and  $r_c = 2.5$ , respectively.

Figure 2 shows the outcome of the experiment: the mean acceptance probability per particle for the per particle and trivial partitions as a function of the number of particles. The acceptance probability for the trivial partition clearly deteriorates with system size. On the other hand, the acceptance probability for the per particle partition is independent of system size. In fact, the acceptance probability per particle is equal to one to within round off error. This result seems

to defy intuition since the particles experience Lennard-Jones interaction. But, keep in mind that these interactions are, in fact, short-range due to the cutoff in the Lennard-Jones potential energy. Hence, the change in energy induced by per particle Verlet moves is independent of system size.

### 3.4 Autocorrelation of Lennard-Jones Dumbbells

A rigid dumbbell is a type of molecule that involves a holonomic constraint. It consists of a pair of particles constrained to a fixed distance from one another. The constraint arises when the spring joining a flexible dumbbell infinitely stiffens. Consider  $n$  identical dumbbells where particles in separate dumbbells interact via a Lennard-Jones potential energy (28).

For the numerical experiment, we simulate the dumbbells in a simulation box of length  $\ell$  and  $d = 2$  dimensions as before. We set the system's density  $\rho = 0.998$  and temperature  $\mathcal{T} = 3.0$  (units are dimensionless as described earlier). We also fix the number of dumbbells to  $n = 30$  and the length of each dumbbell to  $\ell_0 = 1$ . If the positions of the  $i$ th pair of particles describing the  $i$ th dumbbell are  $\mathbf{q}_{i,1}$  and  $\mathbf{q}_{i,2}$ , then the constraint function associated to the  $i$ th dumbbell is given by:

$$g_i(\mathbf{q}) = |(\mathbf{q}_{i,1} - \mathbf{q}_{i,2}) \bmod \ell|^2 - \ell_0^2, \quad i = 1, \dots, n.$$

The size of the simulation box is  $\ell = (2n/\rho)^{1/2} \approx 7$ . The cutoff distance in (27) is set at  $r_c = 3.0$ . The initial positions of the dumbbells are chosen randomly in the simulation box, but with no overlap. The initial velocities are sampled from the Maxwell distribution constrained to be tangent to the constraint manifold at the initial positions and temperature. The thermostat parameter is set to  $\gamma = 1.0$ .

To quantify the accuracy of the numerical method, we use the Metropolized integrator based on a per dumbbell partition. We again use the relative Richardson error defined in (29) to estimate the rate of convergence of the method. Figure 3 shows the velocity autocorrelation that we wish to approximate over the time-interval  $[0, 1]$ . It is noticeably different from the velocity autocorrelation in the case of the Lennard-Jones cluster without constraints. The figure also shows a plot of the Richardson error as a function of time-stepsize. The rate of convergence appears to be approximately  $O(h^2)$ .

## 4 Conclusions

This paper showed how thinking probabilistically helps to design good integrators for SDEs arising in molecular dynamics. The paper brought ideas from Monte Carlo into molecular dynamics, to obtain a Metropolized integrator that is unconditionally stable, pathwise accurate, and still explicit. While the examples and theory in the paper focused on Langevin dynamics, the methodology can be extended to other thermostats. The patch we propose is simple and, as we showed, its computational overhead is minimum compared to an ‘unpatched’ integrator.

An open question about the Metropolized integrator is its convergence rate to equilibrium. In general, it is not expected that the Metropolized integrator inherits all of the mixing properties of the exact solution to the SDE. The main reason is conditional stability of the underlying Verlet integrator that generates proposal moves. Indeed for any time-stepsize one can find an energy value above which the drift in this integrator gives proposed moves that increase the energy, in contrast to the exact drift in the SDE which always centers the solution towards lower energy values. Since higher energy values have a lower equilibrium probability weight, these proposed moves are typically rejected. While these rejections ensure that the Metropolized integrator is ergodic, at high energy values they prevent the integrator from inheriting all of the mixing properties of the true solution.

This issue has been addressed for the MALA algorithm in the overdamped limit of Langevin dynamics [6]. It turns out that MALA converges to its equilibrium distribution at an exponential rate up to terms exponentially small in time-stepsize. However, in the overdamped limit positions are no longer differentiable, momentum is no longer present, and the MALA algorithm does not involve momentum flips. Intuitively one expects these momentum flips to reduce stagnation at high energy values, and hence, enhance the mixing rate. Future research will investigate the effect of these momentum flips to this mixing rate.

Another open question concerns the acceptance probability of the Metropolized integrator as the dimension tends to  $\infty$ . The numerical experiment in Figure 2 indicates that the acceptance probability of the Metropolized integrator based on global Verlet moves scales as  $\mathcal{O}(n^{-1/6})$  where  $n$  is the number of particles. Thus, to obtain an  $\mathcal{O}(1)$  acceptance probability the time stepsize should be proportional to  $n^{-1/6}$ , and the integrator would require  $\mathcal{O}(n^{1/6})$  steps to traverse phase space. This scaling property would imply that the Metropolized integrator is more efficient at making  $\mathcal{O}(1)$  moves in state space as compared with the  $\mathcal{O}(n^{1/4})$  and  $\mathcal{O}(n^{1/3})$  scalings of respectively hybrid Monte-Carlo and MALA [5]. This question will also be investigated in future work.

**Acknowledgements** We wish to thank Gerard Ben-Arous, Weinan E, Martin Hairer, Mikael Rechtsman, Christof Schütte, Andrew Stuart, Maddalena Venturoli, and Jonathan Weare for stimulating discussions. The research of NBR was supported in part by NSF Fellowship DMS-0803095. The research of EVE was supported in part by NSF grants DMS-0718172 and DMS-0708140, and ONR grant N00014-04-1-6046.

## Appendix

*Proof of Corollary 2.5.* We prove this estimate for the equilibrium correlation of any Lipschitz function  $g \in C^{0,1}(\Omega, \mathbb{R})$ . This assumption includes the special case of a scalar velocity autocorrelation function. Ergodicity of the Metropolized integrator (see Theorem 2.4) implies that

$$\lim_{N \rightarrow \infty} \frac{1}{N} \sum_{k=1}^N g(\mathbf{X}_{\lfloor t_k/h \rfloor}) g(\mathbf{X}_{\lfloor (t_k+\tau)/h \rfloor}) = \langle g(\mathbf{X}_{\lfloor t/h \rfloor}) g(\mathbf{X}_{\lfloor (t+\tau)/h \rfloor}) \rangle$$

for any  $t \geq 0$ . (Recall, that the angle brackets denote a double average with respect to initial conditions distributed according to the equilibrium distribution of (18) and realizations of the Wiener process.) Thus, we wish to estimate:

$$\begin{aligned} \epsilon_h &\stackrel{\text{def}}{=} \left| \langle g(\mathbf{X}_{\lfloor t/h \rfloor}) g(\mathbf{X}_{\lfloor (t+\tau)/h \rfloor}) \rangle - \langle g(\mathbf{Y}(t)) g(\mathbf{Y}(t + h \lfloor \tau/h \rfloor)) \rangle \right| \\ &= \left| \langle g(\mathbf{x})(g(\mathbf{X}_{\lfloor \tau/h \rfloor}) - g(\mathbf{Y}(h \lfloor \tau/h \rfloor))) \rangle \right|. \end{aligned}$$

By the Cauchy-Schwarz inequality,

$$\epsilon_h \leq C_g \left( \int_{\Omega} |\mathbb{E}^{\mathbf{x}} \{g(\mathbf{X}_{\lfloor \tau/h \rfloor}) - g(\mathbf{Y}(h \lfloor \tau/h \rfloor))\}|^2 d\mu \right)^{1/2},$$

where  $C_g = (\int_{\Omega} |g(\mathbf{x})|^2 d\mu)^{1/2}$ . By Jensen's inequality,

$$\epsilon_h \leq C_g \left( \mathbb{E}^{\mu} \left\{ |g(\mathbf{X}_{\lfloor \tau/h \rfloor}) - g(\mathbf{Y}(h \lfloor \tau/h \rfloor))|^2 \right\} \right)^{1/2}.$$

The Lipschitz assumption on  $g$  implies,

$$|g(\mathbf{x}) - g(\mathbf{y})| \leq L_g |\mathbf{x} - \mathbf{y}|$$

for some constant  $L_g > 0$  and for every  $\mathbf{x}, \mathbf{y} \in \Omega$ . Hence,

$$\epsilon_h \leq L_g C_g \left( \mathbb{E}^\mu \left\{ |\mathbf{X}_{\lfloor \tau/h \rfloor} - \mathbf{Y}(h \lfloor \tau/h \rfloor)|^2 \right\} \right)^{1/2}.$$

Pathwise convergence of the Metropolized integrator (see Theorem 2.3) implies

$$\left( \mathbb{E}^\mu \left\{ |\mathbf{X}_{\lfloor \tau/h \rfloor} - \mathbf{Y}(h \lfloor \tau/h \rfloor)|^2 \right\} \right)^{1/2} \leq C(T)h.$$

From which it follows, that the accuracy of the Metropolized integrator in computing the equilibrium correlation in  $g$  is  $O(h)$  with a prefactor that depends on the function  $g$ .  $\square$

## References

- [1] E. Akhmatskaya and S. Reich, *GSHMC: An efficient method for molecular simulation*, J. Comput. Phys. **227** (2008), 4937–4954.
- [2] M. P. Allen and D. J. Tildesley, *Computer simulation of liquids*, Clarendon Press, 1987.
- [3] H. C. Andersen, *Molecular dynamics simulations at constant pressure and/or temperature*, J. Chem. Phys. **72** (1980), 2384.
- [4] G. Benetin and A. Giorgilli, *On the Hamiltonian interpolation of near to the identity symplectic mappings with applications to symplectic integration algorithms*, J. Statist. Phys. **74** (1994), 1117–1143.
- [5] A. Beskos, N. S. Pillai, G. O. Roberts, J. M. Sanz-Serna, and A. M. Stuart, *Optimal tuning of hybrid Monte-Carlo*, arXiv:1001.4460, 2010.
- [6] N. Bou-Rabee, M. Hairer, and E. Vanden-Eijnden, *Non-asymptotic mixing of the MALA algorithm*, arXiv:1008.3514v1 [math.PR], 2010.
- [7] N. Bou-Rabee and H. Owhadi, *Stochastic variational integrators*, IMA J. of Numer. Anal. **29** (2009), 421–443.
- [8] N. Bou-Rabee and E. Vanden-Eijnden, *Reconciling Monte Carlo and molecular dynamics*, Preprint, 2009.

- [9] N. Bou-Rabee and E. Vanden-Eijnden, *Pathwise accuracy and ergodicity of Metropolized integrators for SDEs*, CPAM **63** (2010), 655–696.
- [10] A. Brünger, C. L. Brooks, and M. Karplus, *Stochastic boundary conditions for molecular dynamics simulations of ST2 water*, Chem. Phys. Lett. **105** (1984), 495–500.
- [11] G. Bussi, D. Donadio, and M. Parrinello, *Canonical sampling through velocity rescaling*, J. Chem. Phys. **126** (2007), 014101.
- [12] G. Bussi and M. Parrinello, *Stochastic thermostats: Comparison of local and global schemes*, Computer Physics Communications **179** (2008), 26–29.
- [13] E. Cancés, F. Legoll, and G. Stoltz, *Theoretical and numerical comparison of some sampling methods for molecular dynamics*, Mathematical Modelling and Numerical Analysis **41** (2007), 351–389.
- [14] G. Ciccotti, T. Lelièvre, and E. Vanden-Eijnden, *Projections of diffusions on submanifolds: Application to mean force computation*, CPAM **61** (2008), 0001–0039.
- [15] W. E and D. Li, *The Andersen thermostat in molecular dynamics*, CPAM **61** (2008), 96–136.
- [16] W. Fong, *Multi-scale methods in time and space for particle simulations*, Ph.D. thesis, Stanford University, 2009.
- [17] W. Fong, E. Darve, and A. Lew, *Stability of asynchronous variational integrators*, J. Comput. Phys. **227** (2008), 8367–8394.
- [18] D. Frenkel and B. Smit, *Understanding molecular simulation: From algorithms to applications, second edition*, Academic Press, 2002.
- [19] J. Goodman and A. Sokal, *Multigrid Monte Carlo method: Conceptual foundations*, Phys. Rev. D **40** (1989), 2035–2071.
- [20] E. Hairer, C. Lubich, and G. Wanner, *Geometric numerical integration*, Springer Series in Computational Mathematics, vol. 31, Springer, 2006.
- [21] C. Hartmann, *An ergodic sampling scheme for constrained Hamiltonian systems with applications to molecular dynamics*, J. Stat. Phys. **130** (2008), 687–712.

- [22] D. J. Higham, X. Mao, and A. M. Stuart, *Strong convergence of Euler-type methods for nonlinear stochastic differential equations*, SIAM J. Numer. Anal. **40** (2002), 1041–1063.
- [23] J. A. Izaguirre, D. P. Catarella, J. M. Wozniak, and R. D. Skeel, *Langevin stabilization of molecular dynamics*, J. Chem. Phys. **114** (2001), 2090.
- [24] B. Leimkuhler, E. Noorizadeh, and F. Theil, *A gentle stochastic thermostat for molecular dynamics*, J. Stat. Phys. **135** (2009), 261–277.
- [25] B. Leimkuhler and S. Reich, *Simulating Hamiltonian dynamics*, Cambridge Monographs on Applied and Computational Mathematics, Cambridge University Press, 2004.
- [26] B. Leimkuhler and R. Skeel, *Symplectic numerical integrators in constrained Hamiltonian systems*, JCP **112** (1994), 117–125.
- [27] T. Lelièvre, M. Rousset, and G. Stoltz, *Langevin dynamics with constraints and computation of free energy differences*, arXiv:1006.4914v1, 2010.
- [28] A. Lew, J. E. Marsden, M. Ortiz, and M. West, *Asynchronous variational integrators*, Arch. Ration. Mech. An. **167** (2003), 85–145.
- [29] D. Li, *On the rate of convergence to equilibrium of the Andersen thermostat in molecular dynamics*, J. Stat. Phys. **129** (2007), 265–287.
- [30] J. S. Liu and Y. N. Wu, *Generalised Gibbs sampler and multigrid Monte Carlo for Bayesian computation*, Biometrika **87** (2000), 353–369.
- [31] Q. Ma, J. A. Izaguirre, and R. D. Skeel, *VERLET-I/R-RESPA/IMPULSE is limited by nonlinear instabilities*, SIAM J. Sci. Comput. **24** (2003), 1951–1973.
- [32] J. C. Mattingly, N. S. Pillai, and A. M. Stuart, *Diffusion limits of the random walk Metropolis algorithm in high dimensions*, arXiv:1003.4306, 2010.
- [33] K. L. Mengersen and R. L. Tweedie, *Rates of convergence of the Hastings and Metropolis algorithms*, Ann. Stat. **24** (1996), 101–121.
- [34] N. Metropolis, A. W. Rosenbluth, A. H. Teller, and E. Teller, *Equations of state calculations by fast computing machines*, J. Chem. Phys. **21** (1953), 1087–1092.

- [35] G. N. Milstein and M. V. Tretyakov, *Numerical integration of stochastic differential equations with nonglobally Lipschitz coefficients*, SIAM J. Numer. Anal. **43** (2005), 1139–1154.
- [36] J. Moser, *Lectures on Hamiltonian systems*, vol. 81, Mem. AMS, 1968.
- [37] S. Reich, *Backward error analysis for numerical integrators*, SIAM J. Numer. Anal. **36** (1999), 1549–1570.
- [38] G. O. Roberts and J. S. Rosenthal, *Optimal scaling of discrete approximations to Langevin diffusions*, J. Roy. Statist. Soc. Ser. B **60** (1998), 255–268.
- [39] G. O. Roberts and R. L. Tweedie, *Geometric convergence and central limit theorems for multidimensional Hastings and Metropolis algorithms*, Biometrika **1** (1996), 95–110.
- [40] J. Ryckaert, G. Ciccotti, and H. Berendsen, *Numerical integration of the Cartesian equations of motion of a system with constraints: Molecular dynamics of n-alkanes*, JCP **23** (1977), 327–341.
- [41] A. A. Samoletov, M. A. Chaplain, and C. P. Dettmann, *Thermostats for “slow” configurational modes*, J. Stat. Phys. **128** (2008), 1321–1336.
- [42] A. Scemama, T. Lelièvre, G. Stoltz, E. Cancés, and M. Caffarel, *An efficient sampling algorithm for variational Monte Carlo*, J. Chem. Phys. **125** (2006), 114105.
- [43] T. Schneider and E. Stoll, *Molecular-dynamics study of a three-dimensional one-component model for distortive phase transitions*, Physical Review B **17** (1978), 1302–1322.
- [44] G. Stoltz, *Some mathematical methods for molecular and multiscale simulation*, Ph.D. thesis, Ecole Nationale des Ponts et Chaussées, 2007.
- [45] D. Talay, *Simulation and numerical analysis of stochastic differential systems : a review*, Probabilistic Methods in Applied Physics (P. Krèe and W. Wedig, eds.), vol. 451, Springer-Verlag, Berlin, 1995, pp. 54–96.
- [46] ———, *Stochastic Hamiltonian systems: Exponential convergence to the invariant measure, and discretization by the implicit Euler scheme*, Markov Processes and Related Fields **8** (2002), 1–36.

- [47] D. Talay and L. Tubaro, *Expansion of the global error for numerical schemes solving stochastic differential equations*, Stoch. Anal. Appl. **8** (1990), 94–120.
- [48] M. E. Tuckerman and B. J. Berne, *Stochastic molecular dynamics in systems with multiple time scales and memory friction*, J. Chem. Phys. **95** (1991), 4389–4396.
- [49] M. E. Tuckerman, B. J. Berne, and G. Martyna, *Reversible multiple time scale molecular dynamics*, J. Chem. Phys. **97** (1992), 1990–2001.
- [50] E. Vanden-Eijnden and G. Ciccotti, *Second-order integrators for Langevin equations with holonomic constraints*, Chem. Phys. Lett. **429** (2006), 310–316.
- [51] E. Vanden-Eijnden and M. Venturoli, *Markovian milestoning with Voronoi tessellations*, J. Chem. Phys. **130** (2008), 194101.
- [52] ———, *Exact rate calculations by trajectory parallelization and twisting*, In press, 2009.
- [53] L. Verlet, *Computer “experiments” on classical fluids. I. Thermodynamical properties of Lennard-Jones molecules*, Phys. Rev. **159** (1967), 98–103.

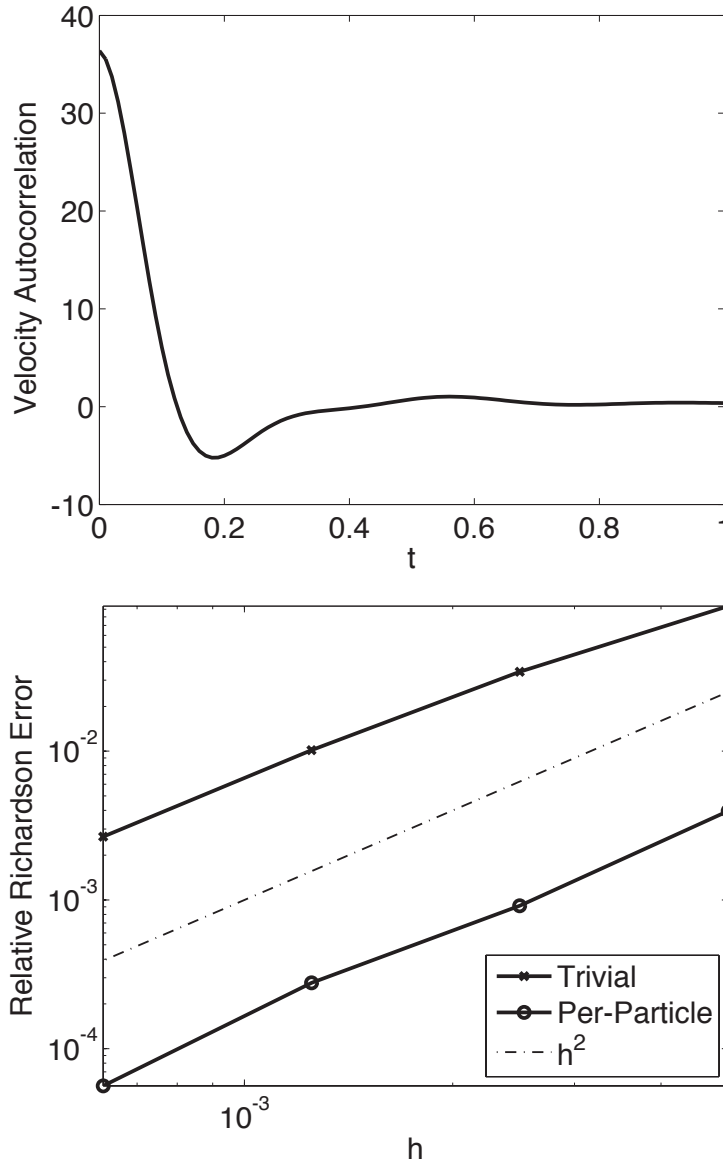


Figure 1: **Autocorrelation of Lennard-Jones Fluid.** The panel on the top shows the velocity autocorrelation function over the time interval  $[0, 1]$ . The panel on the bottom shows a loglog plot of the Richardson error ((29)) of the Metropolized integrator based on trivial and per-particle partitions. The molecular system integrated is the Lennard-Jones fluid with 25 particles in a square box. The dashed line represents a reference slope of  $h^2$ . A total of  $N = 10^8$  samples were used to obtain these empirical estimates. Notice that the Metropolized integrator based on per-particle Verlet moves is about an order of magnitude more accurate than the Metropolized integrator based on global Verlet moves.

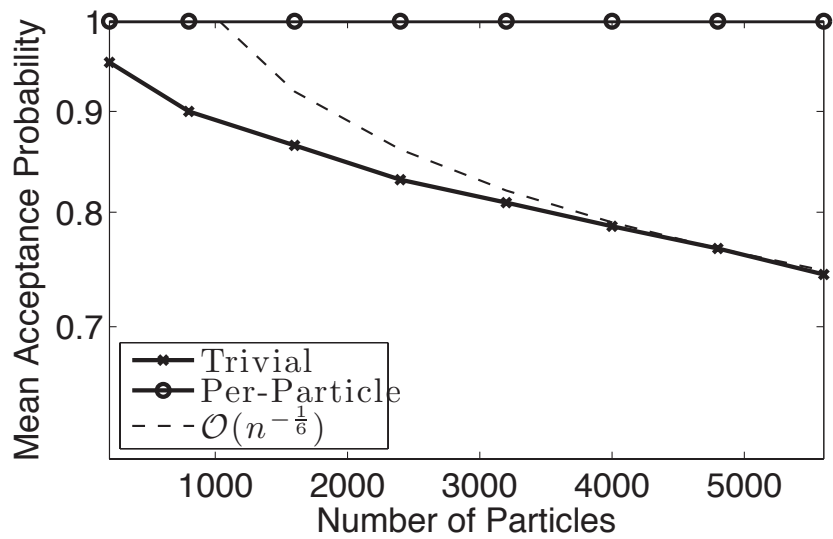


Figure 2: **Mean Acceptance Probability as a Function of System Size.** This figure shows the mean acceptance probability per particle for the integrator (13) based on a trivial and per particle partition. From the plot it is clear that a) the acceptance probability for the integrator based on a per particle partition is independent of system size and b) the acceptance probability for the trivial partition scales like  $n^{-1/6}$  where  $n$  is the number of particles.

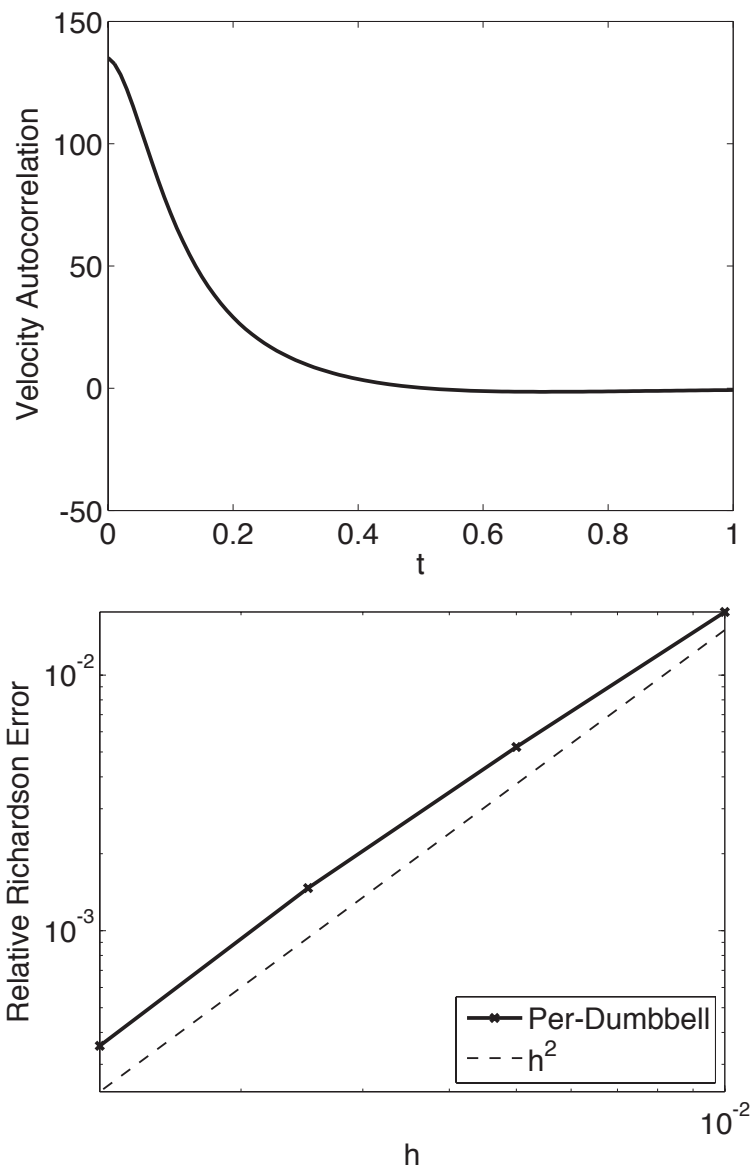


Figure 3: **Autocorrelation of Lennard-Jones Dumbbells.** The panel on the top shows the velocity autocorrelation function. The panel on the bottom shows a loglog plot of an empirical estimate of the Richardson error ((29)) of the Metropolized integrator based on per-dumbbell RATTLE proposed moves. The molecular system integrated is the Lennard-Jones system of 15 dumbbells in a square box. The dashed line represents a reference slope of  $h^2$ . A total of  $N = 10^8$  samples were used to obtain this estimate.